Volume 9, Issue 4, 2019, 4119 - 4125 **ISSN 2069-5837**

Biointerface Research in Applied Chemistry

www.BiointerfaceResearch.com

https://doi.org/10.33263/BRIAC94.119125

Original Research Article **Open Access Journal**

Received: 10.07.2019 / Revised: 04.08.2019 / Accepted:10.08.2019 / Published on-line:15.08.2019

Development of ion-imprinted cryogels for selective removal of arsenic from environmental waters

Hatice Bektaş[1], Müge Andaç [1], Kemal Çetin [2], Tahira Qureshi [3], Adil Denizli [3,*]

[1]Department of Environmental Engineering, Hacettepe University, Ankara, Turkey
[2]Biochemistry Division, Department of Chemistry, Faculty of Science, Necmettin Erbakan University, Konya, Turkey
[3]Biochemistry Division, Department of Chemistry, Hacettepe University, Ankara, Turkey

*corresponding author e-mail address: ***denizli@hacettepe.edu.tr***

ABSTRACT

Arsenic present by nature as metalloid, having transportability in the environment via diverse sources. Because of both natural processes and anthropogenic activities, arsenic is found in environmental water sources. The aim of this study is to design ion-imprinting-based cryogel adsorbents for the removal of arsenic species from environmental waters. Since trivalent arsenic exhibit a high afgfinity for sulfhydryl groups, cysteine-based functional monomer, i.e. MAC, was synthesized and MAC–As(III) complex was prepared. Ion-imprinted polymeric adsorbents were fabricated via cryopolymerization. Elemental analysis studies have shown that the cryogel monolith contains 192.8 μmol/g mol MAC/g polymer. The maximum adsorption capacity of ion-imprinted cryogels at an initial arsenic concentration of 10 ppm was found to be 372.5 μg/g at pH 8.0. Arsenic removal rate of the imprinted cryogels from environmental water sample was determined as 94.8% In the studies carried out for the removal of arsenic from the environmental waters, 94.8% removal efficiency was achieved. Reusability assays of ion-imprinted cryogels were performed and there was no significant decrease in adsorption capacity.

Keywords: *Amino acid-based monomers, arsenic removal, cryogels, ion-imprinted polymers, water treatment.*

1. INTRODUCTION

Arsenic is one of the heavy metals in the environment that are toxic to human beings and other living organisms [1]. Arsenic concentrations found in groundwater of at least 40 countries are higher than 10 μg/L and it is estimated that 200 million people in the world are at risk due to high concentrations of arsenic in drinking water [2,3]. As a result of both natural processes and anthropogenic activities, arsenic is found in environmental waters in different forms. Generally, arsenite species are considered to be 10 and 70 times more toxic than arsenate species and organoarsenic species, respectively [4,5]. The toxicity of arsenite species mainly based on irreversible complexation of them with sulfhydryl groups present in the structure of some amino acids, mainly cysteine [5]. Studies showed that solubility of As(III) is 4 to 10 times higher in water than the solubility of As(V). On the other hand, it has been found that trivalent methylated arsenic species are more toxic than inorganic arsenic due to the fact that they are more effective in causing DNA degradation [6].

Arsenic removal from water sources is still a challenging issue because of conventional removal methods including coagulation and filtration exhibit drawbacks such as lack of regeneration, low treatment efficiencies, high costs or lack of selectivity [7,8]. An alternative method for the removal of arsenic species is selective adsorption via molecular imprinting technology (MIT). MIT enables to prepare polymers with specific binding sites complementary to a target molecule. Ion-imprinted polymers (IIPs) are polymeric systems prepared on the basis of MIT and using an ion as the template. IIPs can be performed in specific and selective removal or detection of heavy metal ions from environmental sources [9,10].

Polymeric systems prepared by cryopolymerization, so-called cryogels, are known with their macroporous structure (10-200 μm), large inter-connected flow channels, low solids content (0.2–20%), low density (around 95% of the volume of dry cryogels is air), low diffusion resistance and low back pressure [13-16]. In the literature, cryogels are utilized in various biotechnological and biomedical applications such as separation and purification technologies, sensor systems, tissue engineering and drug delivery systems [17-22].

Herein, MIT-based cryogel adsorption system was designed for the selective removal of As(III) species from environmental water sources. Since trivalent arsenic has a high affinity for sulfhydryl groups, a polymerizable derivative of cysteine, i.e. N-methacryloyl-(L)-cysteine (MAC), was synthesized and MAC–As(III) complex was prepared. IIPs produced via cryopolymerization were characterized by scanning electron microscopy (SEM), elemental analysis, multi-point Brunauer–Emmett–Teller (BET) method, swelling tests and so on. Optimum adsorption conditions were determined by examining the change in adsorption capacity by changing the parameters such as pH, contact time and flow rate. Selectivity of IIPs towards arsenite species was investigated in the presence of SO_4^{2-}, PO_4^{3-} and NO_3^- ions. IIPs were also performed using environmental water samples to test the selective removal efficiency of IIPs.

2. MATERIALS AND METHODS

2.1. Reagents.

Following chemicals were used as received; methacryloyl chloride, L-cysteine, 2-hydroxyetyhl methacrylate (HEMA), ammonium persulfate (APS), N,N′-methylenebis(acrylamide) (MBAAm) and N,N,N',N'-tetramethyl ethylene diamine (TEMED) were purchased from Sigma Chemical Co. (St. Louis, MO, USA). $NaAsO_2$ as the source of As(III) ion were purchased from Merck (Merck Co., Darmstadt, Germany).

2.2. Preparation of arsenic-monomer complexes.

Firstly, N-methacryloyl-(L)-cysteine (MAC), a polymerizable derivative of cysteine amino acid was synthesized according to the procedure represented in our earlier study [23]. MAC was complexed with arsenic ions with 1:3 mol ratios of As:MAC. Sodium arsenite ($NaAsO_2$) salt was used in order to form complexes of MAC–As(III). 1.0 mmol of $NaAsO_2$ (0.129 g) was dissolved in 15.0 mL of ethanol. 3.0 mmol of solid MAC (0.570 g) was then added to this solution and stirred continuously using a magnetic stirrer at room temperature for 3 h. The resulting arsenic–monomer complex was precipitated, filtered and washed with a 99% solution of ethanol (250 ml) and dried in a vacuum oven at 30ºC for 24 h.

2.3. Fabrication of IIP and NIP cryogels.

The supermacroporous cryogels were prepared by free radical polymerization technique. As(III) imprinted (IIP) cryogels were fabricated as follows: 20.0 mg of MAC–As(III) complex was dissolved in 5.0 mL of deionized water (DW) and 1.3 mL of HEMA monomer was added to this solution (the first solution). Then, 0.283 g of MBAAm was dissolved in 10.0 mL of DW as the second solution and the second solution was mixed with the first one. 20.0 mg of APS (1%, w/v) and 25.0 µL of TEMED (1%, w/v) were added to the solution and stirred for 1 minute. The solution was transferred into plastic syringes (5.0 ml, id. 0.8 cm) with a closed outlet at the bottom and the syringes were kept at -16°C for 24 h for cryopolymerization and then thawed at room temperature, thereby yielding supermacroporous IIP cryogels. The cryogel was washed with 200 mL of DW, then with 50 mM EDTA (pH 4.0) solution to remove the arsenic ions from the cryogel. Non-imprinted (NIP) cryogels were prepared at the same concentration but no adding As(III) ions. The fabricated cryogels were stored in 0.02% sodium azide (NaN_3) solution at 4°C until use.

2.4. Characterization studies.

Raman Spectra were measured in the range of 50−4000 cm^{-1} using a Raman spectrometer (Labram 800 HR, Jobin Yvon, France) in order to determine the formation of MAC–As(III) complex. A He–Ne laser with a 632.8 nm wavelength and Liquid nitrogen-cooled CCD detector were utilized.

The following properties of the cryogels were calculated using the corresponding equations:

Gelation yield: $G\ (\%) = \frac{W_0}{W_m}\ x\ 100$ (1)

Equilibrium swelling degree: $= \frac{W_1 - W_0}{W_0}$ (2)

Macroporosity: $M\ (\%) = \frac{W_1 - W_2}{W_1}\ x\ 100$ (3)

where W_m is total mass (g) of the monomers used for gelation; W_0, W_1 and W_2 represent the weights (g) of dried cryogel samples while W_1 and W_2 are the weights (g) of fully swollen in DW and squeezed cryogel samples, respectively.

Surface and bulk structures of IIP and NIP cryogels were investigated by scanning electron microscopy (SEM). The samples were attached to the aluminum SEM sample plate with a conductive adhesive. Subsequently, the sample surfaces were coated with 200 Å of metallic gold under a vacuum to make the surface conductive. The samples were placed in the SEM sample well and photographed at various magnification rates using a scanning electron microscope (JEOL, JEM 1200 EX, Tokyo, Japan).

The pore volume and average pore diameter of the IIP and NIP cryogels were determined by mercury porosimetry (Carlo Erba Model 200, Milan, Italy). Specific surface areas of the cryogels were determined by the multi-point Brunauer–Emmett–Teller (BET) method using multipoint BET apparatus (Quantachrome, NOVA 2000, USA).

Elemental analysis was performed to determine the amount of MAC in synthesized IIP cryogels. 1.0 mg of cryogels were placed in the aluminum cell of the elemental analyzer (Leco, CHNS-932, USA) and weighed with a sensitivity of ± 0.0001 g. Then, the cryogel samples were placed in the device and carbon, hydrogen, oxygen, nitrogen and sulfur ratios of the samples were determined.

2.5. Optimization of arsenic removal conditions.

Arsenic ion adsorption from aqueous solutions was studied using IIP cryogels. As(III) ion solutions (50 mL) was continuously pumped into the cryogel columns using a peristaltic pump (Ismatec, Zurich, Switzerland). Prior to experimental studies, the cryogel columns were conditioned with 50 mL of DW for 30 min. Effects of initial As(III) concentration (0.05-15 mg/L), flow rate (0.5-3.0 mL/min), medium pH (4.0-9.0) and adsorption time (15-150 min) on As(III) adsorption capacities of the cryogels were investigated.

As(III) ion concentrations in solutions were determined using a flame atomic absorption spectrophotometer (Analyst 800, Perkin Elmer, USA). The amount of As(III) ions adsorbed by IIP cryogels was calculated by the following equation:

$$Q_e = \frac{(C_0 - C_e)\ x\ V}{W} \qquad (4)$$

where Q_e is the amount (µg/g) of arsenic ions adsorbed onto the cryogels, C_0 is the initial arsenic ion concentration (µg/mL), C_e is the equilibrium arsenic ion concentration (µg/mL) in the solution, V is the volume (mL) of the solution while W represents the weight (g) of the cryogel.

2.6. Selectivity studies.

Selectivity of IIP cryogels were investigated in the presence of 5 ppm of competitor anions (NO_3^-, PO_4^{3-} and SO_4^{2-}) in 100 ml of solution. The competitor anions were compared with AsO_2^- oxy-anion in a continuous system at room temperature for 2 h. The concentrations of competitor anions were measured using an ion chromatography system (Dionex, ICS-1000, Dionex Corporation,

USA) while oxy-anion concentrations were measured using an Inductively Coupled Plasma – Mass Spectrometer, ICP-MS (Thermo Elemental X7, Thermo Elemental, Winsford, UK) in the remaining solution. The following terms and equations were utilized in order to investigate the selectivity of the IIP cryogels:

Distribution coefficient: $K_d = \frac{C_i - C_f}{C_f} x \frac{V}{m}$ (5)

Selectivity coefficient: $k = \frac{K_{d\,(template)}}{K_{d\,(competitor)}}$ (6)

Relative selectivity coefficient: $k' = \frac{k_{imprinted}}{k_{non-imprinted}}$ (7)

where C_i (mg/L) is initial and C_f (mg/L) is the final ion concentrations; m (g) is the weight of dry cryogels; and V (mL) is the volume of the solutions.

2.7. Reusability studies,

EDTA solution (50 mM, pH 4.0) was used as a desorption agent for the desorption of arsenic ions adsorbed by the cryogels. Prior to the desorption process, the cryogels were washed with DW to remove impurities and other unbound residues. Desorption was performed with 100 mL of desorption solution at room temperature for 2 h. After desorption, the cryogels we washed with DW again and then re-equilibrated with adsorption buffer. The adsorption-desorption process was performed by reusing the same adsorbent 10 times after regeneration to determine the reusability of IIP cryogels.

2.8. Removal efficiency in an environmental water sample,

The environmental water sample was collected from a mining area located around Ankara, Turkey. The water sample was put in a clean polypropylene bottle and stored at 4 °C. Before use, the sample was filtered through a 0.2 µm membrane. 100 mL of the environmental water sample was taken and treated with IIP cryogels at a flow rate of 1.0 mL/min at room temperature for 2 h. Initial and final ion concentrations were determined using the ICP-MS.

3. RESULTS

3.1. Characterization studies.

Trivalent arsenic has a high affinity for sulfhydryl groups, thereby can bind to reduced cysteine amino acids [24]. Therefore, in this study, MAC was selected as the functional monomer in the selective removal of arsenic ions from environmental water sources. In the literature, studies showed that arsenite forms a complex with three cysteines in proteins in the form of trigonal-pyramidal coordination geometry [25-27]. A model for the complex of MAC–As(III) is shown in Fig. 1.

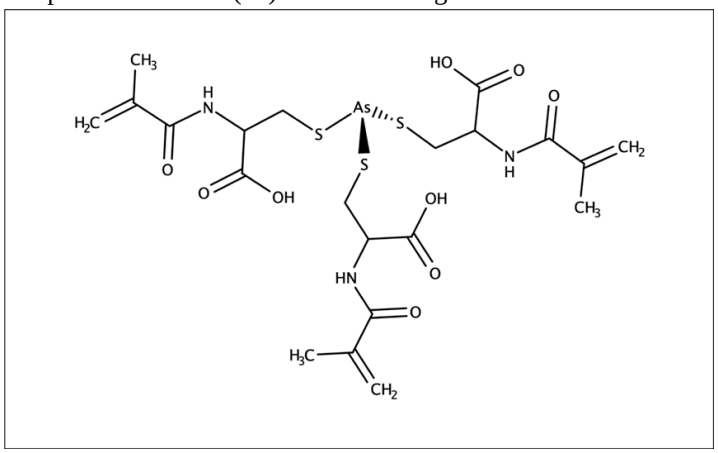

Figure 1. Hypothetical model of the anticipated MAC–As(III) complex.

Raman spectrometry was utilized in order to confirm the formation of the MAC–As(III) complex. Raman spectra of the MAC monomer and MAC–As(III) complex are shown in Fig. 2. The band at 2654.7 cm^{-1} is a characteristic band for S–H stretching for MAC monomer. The band at 3035.1 cm^{-1} is associated with the C–H stretching while the bands at 1259.4 cm^{-1} and 1167.7 cm^{-1} belong to bending of CH_2–S and C–S, respectively. The band at 538 cm^{-1} in the spectrum of MAC–As(III) complex is an indication of As–S bond formation. Furthermore, as a result of As-S bond formation, the characteristic S–H band belonging to the MAC monomer is not seen in the spectrum of the complex [5].

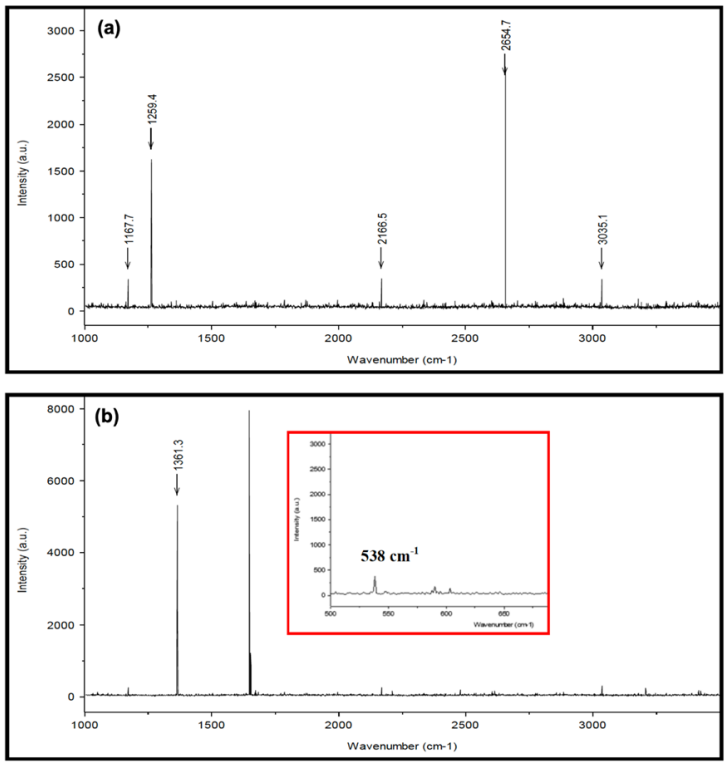

Figure 2. Raman spectra of (a) MAC monomer and (b) MAC–As(III) complex.

Ion-imprinted cryogels were synthesized in order to selective removal of As(III) species from environmental water sources. Non-imprinted cryogels were also synthetized as a control group. Gelation yield, swelling degree, specific surface area and macroporosity of IIPs and NIPs are listed in Table 1. Cryogels were synthesized at very high yield (about 90%). According to SEM images shown in Fig. 3, cryogels have spongy and macroporous structures with a smooth wall surface and interconnected flow channels. Due to their highly macroporous structures, high swelling degrees were observed. The MAC content was 192.8 µmol/g dry cryogel sample. It should be noted

that HEMA, MBAAm, and other chemicals in the cryogel structure do not contain sulfur but only MAC does. The sulfur amount in the cryogel sample was found out using elemental analysis.

Table 1. Physical properties of IIPs and NIPs.

	IIPs	NIPs
Gelation yield (%)	91.2 ± 0.72	90.3 ± 0.68
Specific surface area (m^2/g)	35.6 ± 0.82	24.2 ± 0.95
Macroporosity (%)	65.5 ± 0.38	64.0 ± 0.46
Swelling degree (g H_2O/g cryogel)	10.1 ± 0.12	9.7 ± 0.15

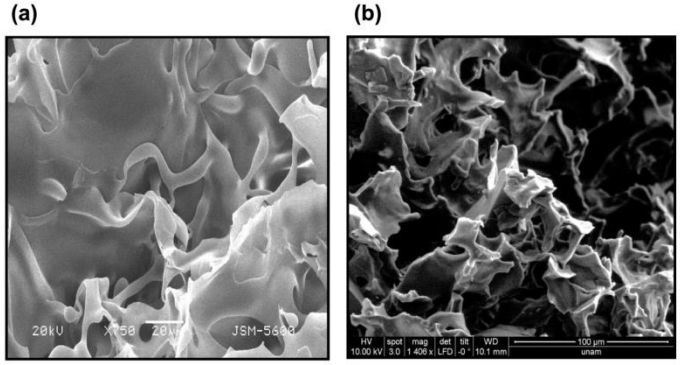

Figure 3. SEM images of (a) IIPs and (b) NIPs.

3.2. Optimization of adsorption conditions.

3.2.1. Effect of pH. The amount of adsorbed As(III) by the cryogels at various pH values was presented in Fig. 4a. After pH 6.0, the concentration of arsenite ion ($H_2AsO_3^-$) increases [28]. In other words, arsenite turns into the anionic form. The As (III) adsorption graph shows a significant increase after pH 5.0. The increase in the amount of adsorption continues up to pH 8.0. This shows that the electrostatic interactions between the MAC monomer and $H_2AsO_3^-$ oxyanions are intense between these two pH values. This can be explained as follows: The isoelectric point of the MAC monomer is 4.9 and the pKa point of the SH group is 8.3. That is, the MAC monomer is in the zwitter ionic form at about pH 5.0, and the SH groups pass into the anionic form by giving a hydrogen atom to the aqueous medium after pH 8.3. In these two pH ranges, the SH groups of the MAC monomer interfere electrostatically with arsenite ($H_2AsO_3^-$) ions. The result is consistent with the literature. The reason for the significant decrease in the adsorption capacity after pH 8.0 is due to the fact that that high pH value weakens the As–S binding [29,30]

3.2.2. Effect of contact time. Effect of adsorption time on As(III) adsorption by ion-imprinted cryogels was investigated at different times from 0 to 150 min and the results were presented in Fig 4b. A higher adsorption rate was observed up to 60 min and after this time the adsorption capacity of the IIP cryogels did not change significantly due to key factors such as; decrease in the As(III) concentration in mobile phase and almost complete occupation of active binding sites of the adsorbent.

3.2.3. Effect of flow rate. Effect of flow rate on As(III) adsorption by IIP cryogels plastic were investigated in the range of 0.5-3.0 mL/min flow rate as shown in Fig. 4c. The maximum As(III) adsorption was observed as 77.4 μg/g polymer at a flow rate of 0.5 mL/min. A decrease in As(III) adsorption onto the IIP cryogels was obtained by increasing flow rate and 18.4 μg/g polymer was observed at a flow rate of 3.0 mL/min. As the flow rate increases, the interaction time through the column decreases. Hence, As(III) ions have less time to diffuse to the pore walls of cryogel and to place into their cavities in the cryogel matrix, thereby a decrement in adsorption capacity is observed.

3.2.4. Effect of initial concentration of arsenic. A significant increment in As(III) adsorption was obtained onto the IIP cryogel columns by increasing As(III) concentration up to 5 ppm, then reached an equilibrium value, which means that the active binding cavities on the IIP cryogels were saturated (Fig. 4d). Maximum As(III) adsorption capacity for the IIP cryogels was calculated as 372.5 μg/g polymer.

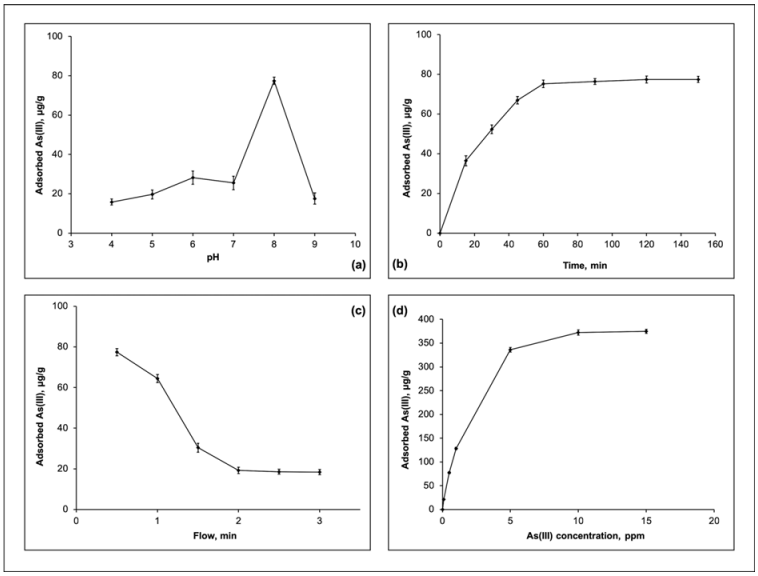

Figure 4. Optimization of As(III) adsorption parameters. (a) Effect of pH (T: 25°C; initial arsenic concentration: 500 μg/L; $m_{dry\ cryogel}$: 0.217 g.) (b) Effect of contact time. (pH 8.0; T: 25°C; initial arsenic concentration: 500 μg/L, $m_{dry\ cryogel}$: 0.217 g.) (c) Effect of flow rate. (pH 8.0; T: 25°C; initial arsenic concentration: 500 μg/L; $m_{dry\ cryogel}$: 0.217 g.) (d) Effect of initial concentration. (pH 8.0; T: 25°C; $m_{dry\ cryogel}$: 0.217 g.).

3.3. Adsorption isotherms.

Adsorption proceeds until a balance is formed between the concentrations of the substance deposited on the adsorbent surface and the substance remaining in the solution. Adsorption isotherms are the mathematical expressions used to describe the relation between the concentration of ions in the solution and the number of ions adsorbed to the solid phase in equilibrium [31]. Langmuir isotherm model and Freundlich isotherm model in their non-linear forms were utilized in order to describe the equilibrium data [32-35].

Langmuir: $$Q_e = \frac{Q_{max} K_L C_e}{1 + K_L C_e} \quad (8)$$

Freundlich: $$Q_e = K_F\, C_e^{1/n} \quad (9)$$

where Q_e (mg/g) and Q_{max} (mg/g) are the adsorbed amount of As(III) by cryogels and maximum adsorption capacity of the cryogels, respectively; C_e (mg/mL) is the equilibrium As(III) concentration; K_L (mL/mg) and K_F are the Langmuir isotherm constant and Freundlich constant related to adsorption capacity of the cryogels, respectively; n is the Freundlich constants related to adsorption intensity of the cryogels. The comparison of the experimental adsorption behavior with Langmuir isotherm and Freundlich isotherm models is shown in Fig. 5. The experimental adsorption behavior of IIP cryogels is consistent with the adsorption behavior modeled by Langmuir isotherm model. The maximum adsorption capacity (0.372 mg/g) obtained as a result of experiments is also very close to the calculated Langmuir

adsorption capacity (0.392 mg/g). According to data, the adsorbed As(III) ions onto the IIP cryogels exhibit a monolayer adsorption behavior.

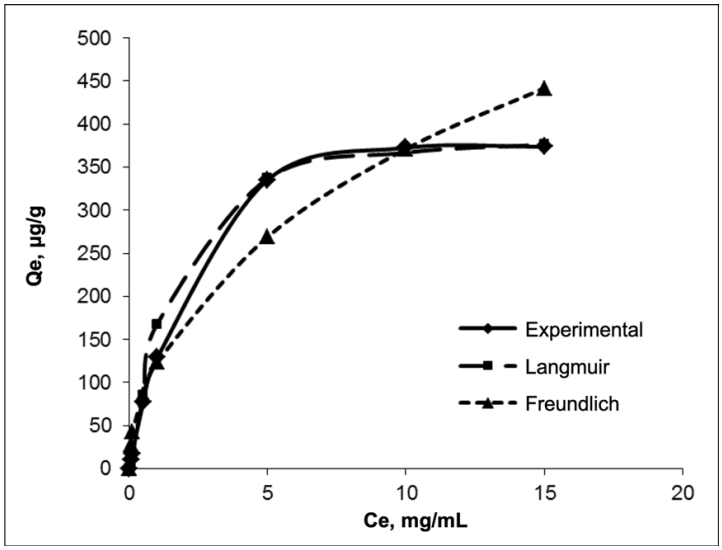

Figure 5. Experimental data of absorbed As(III) on the IIPs compared to Langmuir and Freundlich isotherms.

3.4. Selectivity studies.

Selectivity for As(III) binding of the ion-imprinted and non-imprinted cryogels was investigated using NO_3^-, PO_4^{3-} and SO_4^{2-}. The selectivity coefficient, k, is a criterion of the specificity of the binding regions of the IIPs. When the k values for IIPs and NIPs were compared, it is observed that they are higher for IIPs than the ones for the NIPs. As shown in Table 2, k' values are greater than 1.0; this means that the IIPs show a specific affinity for As (III).

Table 2. *k* and *k'* coefficients for IIPs and NIPs.

	Ion-imprinted cryogels	Non-imprinted cryogels	
Ions	k	k	k'
As(III)	–	–	–
PO_4^{3-}	49.43	6.50	7.60
SO_4^{2-}	37.41	7.0	5.35
NO_3^-	47.05	9.05	5.20

The removal efficiency of As(III) species by cryogels from environmental water samples was also examined under the optimum experimental adsorption conditions and the data were given in Table 3. The removal efficiency of As(III) was found to be 94.8% in the presence of the metal ions listed in Table 3.

Table 3. Removal efficiency from an environmental water sample.

Ion species	Initial concentration in solution (ppb)	Amount of adsorbed ions (ppb)	Removal ratio (%)
Arsenic	21.3	20.2	94.8
Lithium	35.2	0.8	2.3
Boron	660.7	28.7	4.3
Aluminium	69.1	6.0	8.7
Gold	3.9	1.7	43.6
Mercury	9.3	4.3	46.2
Lead	4.8	1.5	31.3
Iron	128.1	23.3	18.2
Zinc	84.9	24.5	28.9
Gallium	1.9	0.8	42.1
Germanium	1.3	0.1	7.7
Selenium	3.8	1.1	28.9
Rubidium	2.9	0.2	6.9
Strontium	338	40.5	12.0
Molybdenum	7.3	0.2	2.7
Palladium	1.0	0.1	10.0
Tin	2.5	0.7	28.0
Barium	54.3	16.9	31.1

3.5. Reusability of adsorbents.

The adsorption-desorption process was performed by reusing the same adsorbent 10 times after regeneration to determine the reusability of IIP cryogels. Desorption has reached equilibrium within 30 minutes due to the interconnected supermacroporous structure of the cryogels. As seen in Fig. 6, high desorption ratios up to 97% and no significant reduction in arsenic adsorption capacity were observed. Hence, it can be concluded that cryogels prepared via MIT provide high stability and can be utilized a couple of times as adsorbent in arsenic removal processes.

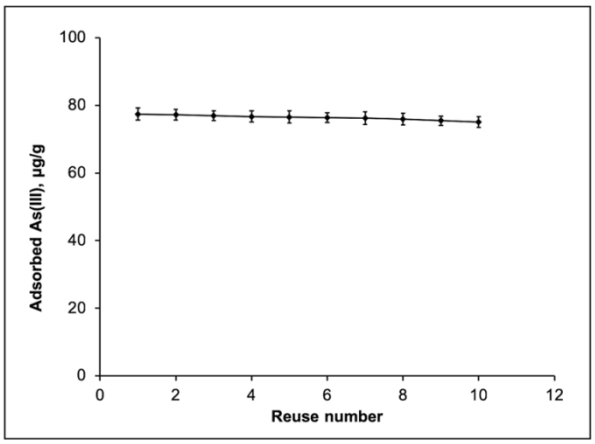

Figure 6. Reusability of the ion-imprinted cryogels. Initial As(III) concentration: 500 µg/mL; flow rate: 0.5 mL/min; temperature: 25°C.

4. CONCLUSIONS

Herein, we designed cryogel systems as an alternative adsorbent for removal of arsenic species by combining outstanding mechanical properties and macroporous structures of cryogels with excellent selectivity of ion-imprinting technology. Trivalent arsenic species have a high affinity for sulfhydryl groups. Therefore, cysteine-based functional monomer, i.e. MAC, was prepared and MAC–As(III) complex was formed for imprinting process. Optimum adsorption conditions were determined by varying the factors such as medium pH, contact time, flow rate and initial arsenic concentration. The maximum adsorption capacity of ion-imprinted cryogels at an initial arsenic concentration of 10 ppm was calculated as 372.5 µg/g polymer at pH 8.0. As a result of the environmental water study with cryogels, As removal rate of IIP was determined as 94.8%. Their outstanding adsorption capacities encourage further expansion of adsorption technologies towards the attainment of tolerable As levels in water sources. That the arsenic imprinted cryogels are cost-friendly, easy to produce and reusable proffers the opportunity to exploit this new adsorbent in the removal of arsenic species from environmental water sources.

5. REFERENCES

1. Jomova, K.; Jenisova, Z.; Feszterova, M.; Baros, S.; Liska, J.; Hudecova, D.; Rhodes, C.J.; Valko, M.; Arsenic: Toxicity, Oxidative Stress and Human Disease, *J. Appl. Toxicol.* **2011**, *31*, 95–107, https://doi.org/10.1002/jat.1649.
2. Khairul, I.; Wang, Q.Q.; Jiang, Y.H.; Wang, C.; Naranmandura, H. Metabolism, Toxicity and Anticancer Activities of Arsenic Compounds. *Oncotarget.* **2017**, *8*, 23905, https://doi.org/10.18632/oncotarget.14733.
3. Ravenscroft, P.; Brammer, H.; Richards, K. *Arsenic Pollution : A Global Synthesis*; Wiley-Blackwell: Chichester, United Kingdom, 2009; https://doi.org/10.1002/9781444308785.
4. Tangahu, B.V.; Sheikh, A.S.R.; Basri, H.; Idris, M.; Anuar, N.; Mukhlisin, M. A Review on Heavy Metals (As, Pb, and Hg) Uptake by Plants through Phytoremediation. *Int. J. Chem. Eng.* **2011,** *2011*, 1–31,. http://dx.doi.org/10.1155/2011/939161.
5. Teixeira, M.C.; Ciminelli, V.S.T.; Dantas, M.S.S.; Diniz, S.F.; Duarte, H.A. Raman Spectroscopy and DFT Calculations of As(III) Complexation with a Cysteine-Rich Biomaterial. *J. Colloid Interface Sci.* **2007**, *315*, https://doi.org/10.1016/j.jcis.2007.06.041.
6. Vaclavikova, M.; Gallios, G.P.; Hredzak, S.; Jakabsky, S. Removal of Arsenic from Water Streams: An Overview of Available Techniques. *Clean Technol. Environ. Policy.* **2008**, *10*, 89–95,. https://doi.org/10.1007/s10098-007-0098-3.
7. Önnby, L.; Pakade, V.; Mattiasson, B.; Kirsebom, H. Polymer Composite Adsorbents Using Particles of Molecularly Imprinted Polymers or Aluminium Oxide Nanoparticles for Treatment of Arsenic Contaminated Waters. *Water Res.* **2012**, *46*, 4111–4120, https://doi.org/10.1016/j.watres.2012.05.028.
8. Mudhoo, A.; Sharma, S.K.; Garg, V.K.; Tseng, C.H. Arsenic: An Overview of Applications, Health, and Environmental Concerns and Removal Processes. *Crit. Rev. Environ. Sci. Technol.* **2011,** *41*, 435–519, https://doi.org/10.1080/10643380902945771.
9. Tamahkar, E.; Bakhshpour, M.; Andaç, M.; Denizli, A. Ion Imprinted Cryogels for Selective Removal of Ni(II) Ions from Aqueous Solutions. *Sep. Purif. Technol.* **2017**, *179*, 36–44,. https://doi.org/10.1016/j.seppur.2016.12.048.
10. Ahmad, I.; Siddiqui, W.A.; Qadir, S.; Ahmad, T.; Synthesis and Characterization of Molecular Imprinted Nanomaterials for the Removal of Heavy Metals from Water. *J. Mater. Res. Technol.* **2018**, *7*, 270–282, https://doi.org/10.1016/j.jmrt.2017.04.010.
11. Wu, P.; Yan, X.P. A Simple Chemical Etching Strategy to Generate "Ion-Imprinted" Sites on the Surface of Quantum Dots for Selective Fluorescence Turn-on Detecting of Metal Ions. *Chem. Commun.* **2010**, *46*, 7046, https://doi.org/10.1039/c0cc01762k.
12. Erdem, Ö.; Saylan, Y.; Andaç, M.; Denizli, A. Molecularly Imprinted Polymers for Removal of Metal Ions: An Alternative Treatment Method. *Biomimetics.* **2018**, *3*, 38, https://doi.org/10.3390/biomimetics3040038.
13. Özgür, E.; Bereli, N.; Türkmen, D.; Ünal, S.; Denizli, A. PHEMA Cryogel for In-Vitro Removal of Anti-DsDNA Antibodies from SLE Plasma. *Mater. Sci. Eng. C.* **2011**, *31*, 915–920, https://doi.org/10.1016/j.msec.2011.02.012.
14. Lazzari, L.K.; Zampieri, V.B.; Neves, R.M.; Zanini, M.; Zattera, A.J.; Baldasso, C. A Study on Adsorption Isotherm and Kinetics of Petroleum by Cellulose Cryogels. *Cellulose.* **2019**, *26*, 1231–1246, https://doi.org/10.1007/s10570-018-2111-x.
15. Bakhshpour, M.; Idil, N.; Perçin, I.; Denizli, A. Biomedical Applications of Polymeric Cryogels. *Appl. Sci.* **2019,** *9*, 553-575.
16. Uzunoğlu, G.; Çimen, D.; Bereli, N.; Çetin, K.; Denizli, A. Cholesterol Removal from Human Plasma with Biologically Modified Cryogels. *J. Biomater. Sci. Polym. Ed.* **2019** *30*, 1276-1290, https://doi.org/10.1080/09205063.2019.1627652
17. Çetin, K.; Denizli, A. Immunoaffinity Microcryogels for Purification of Transferrin. *J. Chromatogr. B.* **2019**, *1114–1115*, 5–12, https://doi.org/10.1016/j.jchromb.2019.03.017.
18. Singh, A.; Shiekh, P.A.; Das, M.; Seppälä, J.; Kumar, A. Aligned Chitosan-Gelatin Cryogel-Filled Polyurethane Nerve Guidance Channel for Neural Tissue Engineering: Fabrication, Characterization, and In Vitro Evaluation. *Biomacromolecules.* **2019**, *20*, 662–673, https://doi.org/10.1021/acs.biomac.8b01308.
19. Saylan, Y.; Akgönüllü, S.; Yavuz, H.; Ünal, S.; Denizli, A. Molecularly Imprinted Polymer Based Sensors for Medical Applications. *Sensors.* **2019**, *19*, 1279, https://doi.org/10.3390/s19061279 .
20. Çetin, K.; Alkan, H.; Bereli, N.; Denizli, A. Molecularly Imprinted Cryogel as a PH-Responsive Delivery System for Doxorubicin. *J. Macromol. Sci. Part A Pure Appl. Chem.* **2017**, *54*, 502–508, https://doi.org/10.1080/10601325.2017.1320757.
21. Bakhshpour, M.; Bereli, N.; Şenel, S. Preparation and characterization of thiophilic cryogels with 2-mercapto ethanol as the ligand for IgG purification. *Colloids. Surfaces. B.* **2014**, *113*, 261-268, https://doi.org/10.1016/j.colsurfb.2013.09.018**.**
22. Derazshamshir, A.; Aşır, S.; Göktürk, I.; Ektirici, S.; Yılmaz, F.; Denizli, A. Polymethacryloyl-L-Phenylalanine [PMAPA]-Based Monolithic Column for Capillary Electrochromatography. *J. Chromatogr. Sci.* **2019**, 1–8, https://doi.org/10.1093/chromsci/bmz047**.**
23. Uzun, L.; Türkmen, D.; Yılmaz, E.; Bektaş, S.; Denizli, A. Cysteine Functionalized Poly(Hydroxyethyl Methacrylate) Monolith for Heavy Metal Removal. *Colloids Surfaces A Physicochem. Eng. Asp.* **2008**, *330*, 161–167. https://doi.org/10.1016/J.COLSURFA.2008.07.045.
24. Shen, S.; Li, X.F.; Cullen, W.R.; Weinfeld, M.; Le, X.C. Arsenic Binding to Proteins. *Chem. Rev.* **2013,** *113*, 7769–7792, https://doi.org/10.1021/cr300015c.
25. Chen, B.; Liu, Q.; Popowich, A.; Shen, S.; Yan, X.; Zhang, Q.; Li, X.F.; Weinfeld, M.; Cullen, W.R.; Le, X.C. Therapeutic and Analytical Applications of Arsenic Binding to Proteins. *Metallomics* **2015,** *7*, 39–55, https://doi.org/10.1039/C4MT00222A.
26. Rey, N.A.; Howarth, O.W.; Pereira-Maia, E.C., Equilibrium Characterization of the As(III)–Cysteine and the As(III)–Glutathione Systems in Aqueous Solution. *J. Inorg. Biochem.* **2004**, *98*, 1151–1159, https://doi.org/10.1016/j.jinorgbio.2004.03.010.
27. Brian, T.F.; Craig, P.M.; James, E.; Penner-Hahn, A.; Pecoraro, V.L.; Arsenic(III)−Cysteine Interactions Stabilize Three-Helix Bundles in Aqueous Solution. *Inorganic chemistry* **2000**, *39*, https://doi.org/10.1021/ic0010149.
28. Smedley, P.; Kinniburgh, D.G. A review of the Source, Behaviour and Distribution of Arsenic in Natural Waters. *Appl. Geochemistry.*, 17, 517–568, **2002**.
29. Dominguez L., Yue Z., Economy J., Mangun C.L., Design of Polyvinyl Alcohol Mercaptyl Fibers for Arsenite Chelation. *React. Funct. Polym.* **2002**, *53*, 205–215, https://doi.org/10.1016/S0883-2927(02)00018-5.
30. Hao, J.; Han, M.J.; Wang, C.; Meng, X. Enhanced Removal of Arsenite from Water by a Mesoporous Hybrid Material – Thiol-Functionalized Silica Coated Activated Alumina. *Microporous Mesoporous Mater.* **2009**, *124*, 1–7, https://doi.org/10.1016/j.micromeso.2009.03.021.
31. Labrou, N.E.; Clonis, Y.D. The Interaction of Candida Boidinii Formate Dehydrogenase with a New Family of

Chimeric Biomimetic Dye-Ligands. *Arch. Biochem. Biophys.* **1995**, *316*, 169–178, https://doi.org/10.1006/abbi.1995.1025.
32. Langmuir, I. The Constitution and Fundamental Properties of Solids and Liquids. Part I. Solids. *J. Am. Chem. Soc.* **1916**, *38*, 2221–2295, https://doi.org/10.1021/ja02268a002.
33. Langmuir, I. The Adsorption of Gases on Plane Surface of Glass, Mica and Platinum. *J. Am. Chem. Soc.* **1918**, *40*, 1361–1403, https://doi.org/10.1021/ja02242a004.
34. Freundlich, H. Über Die Adsorption in Lösungen. *Zeitschrift für Phys. Chemie.* **1906**, *57*, 385–470, https://doi.org/10.1515/zpch-1907-5723.
35. Chen, X., Modeling of Experimental Adsorption Isotherm Data. *Information.* **2015**, *6*, 14–22, https://doi.org/10.3390/info6010014.